Crystalline transformation and photocatalytic performance of Bi2O3 by yttrium doping

ARTICLE *in* MATERIALS LETTERS · FEBRUARY 2013

Impact Factor: 2.49 · DOI: 10.1016/j.matlet.2012.11.014

Materials Letters 92 (2013) 372–375

Contents lists available at SciVerse ScienceDirect

Materials Letters

journal homepage: www.elsevier.com/locate/matlet

Crystalline transformation and photocatalytic performance of Bi_2O_3 by yttrium doping

Lifeng Yin*, Yunrong Dai, Junfeng Niu

State Key Laboratory of Water Environment Simulation, School of Environment, Beijing Normal University, Beijing 100875, PR China

ARTICLE INFO

Article history:
Received 3 September 2012
Accepted 5 November 2012
Available online 10 November 2012

Keywords:
Semiconductors
Energy storage and conversion
Microstructure
Solar energy materials
Spectroscopy

ABSTRACT

Y (yttrium)-doped Bi_2O_3 was prepared by the solvothermal synthesis method, followed by annealing at high temperature. With the increase of the annealing temperature, the crystalline phase transformed from $Bi_2O_2CO_3$ to β-Bi_2O_3, $Bi_{19}YO_{30}$, α-Bi_2O_3, and $Bi_{15}YO_{24}$; the morphology changed from irregular particles to thin sheets. The photoabsorptivity of these samples for visible light was strengthened compared with pure Bi_2O_3. Among them, the mixture of α-Bi_2O_3 and $Bi_{15}YO_{24}$ anneal at 600 °C showed the highest photocatalytic activity for the degradation of 4-chlorophenol under visible light irradiation (>420 nm). The pseudo-first-order kinetics rates of photocatalytic reactions by using the samples prepared at 200–600 °C were 0.014, 0.018, 0.0407, 0.079, and 0.0969 min^{-1}. The improved photocatalytic activity and photoabsorptivity are ascribed to the modified electron structure, oxygen vacancy, and surface defect induced by Y-doping.

1. Introduction

Semiconductor photocatalysis has been widely studied as a method to solve recent environmental problems, such as air purification, soil remediation, and wastewater treatment. As the most extensively used photocatalyst, TiO_2 is strongly oxidative, chemically stable, and nontoxic [1]. However, it performs photocatalytic activity only under ultraviolet (UV) light irradiation ($\lambda < 385$ nm) because of its broad band gap (3.2 eV) [2]. Therefore, various approaches have been developed to extend the photoabsorptivity of photocatalyst toward the visible light region. Recently, a number of photocatalysts with narrow band gap were developed, such as CdS [3], Fe_2O_3 [4], Bi_2O_3 [5], Bi_5O_7I [6], and $SrTiO_3$ [7]. These photocatalysts are excellent candidates for degrading organic pollutants under excitation of sunlight.

Among them, Bi-based photocatalysts (Bi_2O_3 and its related compounds) have attracted much attention because of their unique photocatalytic performance. Bi-based photocatalysts show high photocatalytic activity due to the Bi^{3+} with S^2-configuration and layer structure [8]. However, the present Bi-based photocatalysts were limited either by the low photocatalytic efficiency or by the inadequate charge separation capacity. To address this issue, much effort has been focused on modifying Bi_2O_3 to improve its photocatalytic performance. Doping Bi_2O_3 with metal atoms, such as Fe [9], Ti [10], V, Pb, and Ag [11], have been used to narrow the band gap of Bi_2O_3. The narrowed band gap facilitates excitation of an electron from the valence band to the conduction band, which improves the photoabsorptivity and photocatalytic activity of Bi_2O_3.

It has been reported the doping of TiO_2 with rare earth ions influences its optical properties and leads to lower band gap energies [12,13]. Besides, it was found the photocatalytic activity of Y-doped TiO_2 is related to its ζ potential [14]. However, the Y-induced influences on the photocatalytic performance of Bi_2O_3 has rarely been reported. Here, we doped Bi_2O_3 with Y (yttrium) to prepare a visible light driven photocatalyst, and investigated the crystalline phase, structure, and morphology transformation during annealing. We found the photoabsorptivity and photocatalytic activity of Y-doped Bi_2O_3 was gradually strengthened with the increase of the annealing temperature. Sequentially, the influences of the crystalline phase and Y-doping content on the photocatalytic activity of Y-doped Bi_2O_3 is discussed. The mechanism of the strengthened photoabsorptivity and photocatalytic activity is proposed as well.

2. Experimental

Synthesis of Y-doped Bi_2O_3: A typical synthesis was as follows: 24.0 mmol $Bi(NO_3)_3 \cdot 5H_2O$ was dissolved in 100 mL pure acetic acid and mixed with 1.8 mmol $Y(NO_3)_3 \cdot 6H_2O$ after adjusting the acidity to $pH < 2$ with concentrated nitric acid. The solution was continuously stirred for 8 h and then transferred to a Teflon-lined crystallization vessel and kept at 150 °C for 24 h. The samples were filtered, collected, and annealed from room temperature to 200, 300, 400, 500, and 600 °C at increasing rate of 10 °C min^{-1}

* Corresponding author. Tel./fax: +86 10 5880 7612.
E-mail addresses: lfyin@bnu.edu.cn, yinlifeng@gmail.com (L. Yin).

0167-577X/$ - see front matter © 2012 Elsevier B.V. All rights reserved.
http://dx.doi.org/10.1016/j.matlet.2012.11.014

and held at the annealing temperature for 3 h. The samples were labeled as BYO200–600 according to the annealing temperatures.

Characterization: The samples were characterized using X-ray diffraction (XRD, D/MAX-2000 with Cu-Kα radiation, Japan) from 10° to 80° with a step size of 0.01°. Field-emission scanning electron microscopy (FE-SEM, S4800, Hitachi, Japan) was used to observe the morphology. The elemental composition was measured by the energy dispersive X-ray (EDX) spectrometry. The photoabsorptivity was analyzed by UV–vis diffuse reflectance spectra (DRS, Cary 500, Varian, USA).

Photocatalytic decomposition: The photocatalytic decomposition experiments were conducted under irradiation by a Xenon lamp (CHF-XM-1000W; Trusttech, China) with a cut-off filter at 420 nm (SCF-S50-42L; Sigma Koki, Japan). A 50 mg photocatalyst sample (BYO200–600 and TiO_2) was scattered in 100 mL of 10 mg L^{-1} 4-chlorophenol aqueous solution with a 150 mL quartz beaker under 30 °C. During irradiation, the solution was sampled every 10 min and centrifuged to precipitate the photocatalyst particles. The samples were analyzed by recording the concentration of 4-chlorophenol with high-performance liquid chromatography (HPLC; Waters 600, USA).

3. Results and discussion

XRD analysis: Fig. 1 shows the XRD patterns for samples BYO200–600. For samples annealed at 200 and 300 °C, the XRD patterns can be indexed as an orthorhombic $Bi_2O_2CO_3$ with space group of Pna21(33) by International Center for Diffraction Data (ICDD, PDF no. 84-1752, marked with "●" in Fig. 1). For samples annealed at 400 °C, a tetragonal β-Bi_2O_3 (P421c(114), PDF no. 78-1793, marked with "▲") phase was observed with several tiny extra peaks from the impurity phase $Bi_{19}YO_{30}$ (Tetragonal, PDF no. 39-0275, marked with "☆"). Annealing at 500 and 600 °C, the β-Bi_2O_3 was transformed into α-Bi_2O_3, and the $Bi_{19}YO_{30}$ was transformed into tetragonal $Bi_{15}YO_{24}$ ($P4_2/nmc$ (137), PDF no. 87-1896, marked with "☆"). Associated with the results of EDX, no Y element was detected in BYO200 and BYO300; the contents of Y in BYO400–600 were 1.2%, 3.7%, and 4.6%, suggesting annealing at high temperature introduces Y dopant into the Bi_2O_3 lattice and forms the secondary phases.

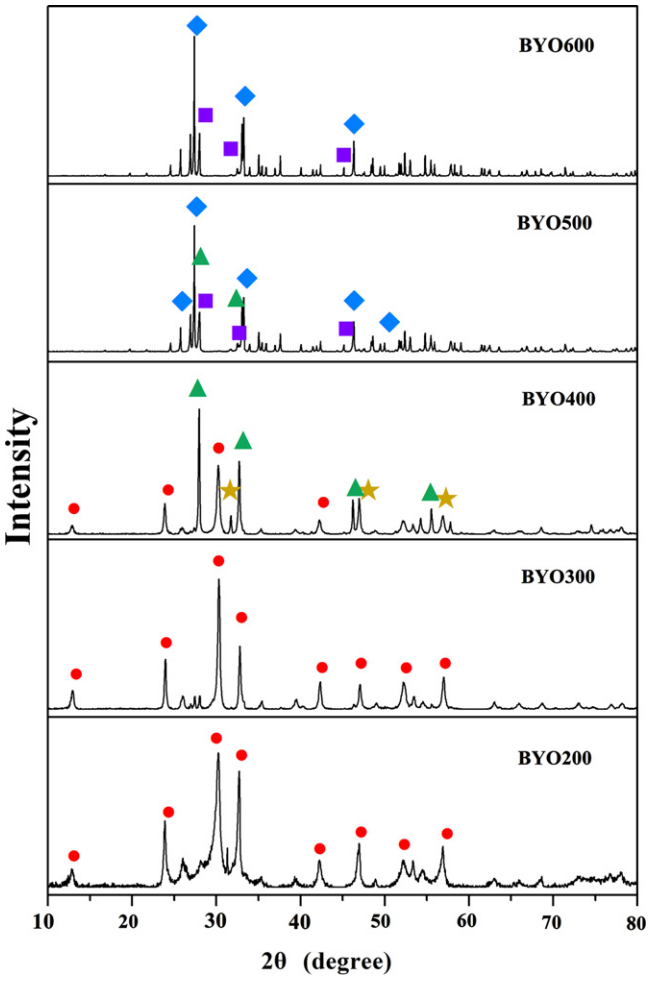

Fig. 1. X-ray diffraction (XRD) patterns of $Bi_2O_2CO_3$ (annealed at 200 °C and 300 °C), Y-doped Bi_2O_3 annealed at 400 °C, 500 °C, and 600 °C (● $Bi_2O_3CO_3$; ▲ β-Bi_2O_3; ★ $Bi_{19}YO_{30}$; ♦ α-Bi_2O_3; and ■ $Bi_{15}YO_{24}$).

Morphology and microstructure: Fig. 2(a)–(d) shows the morphological variation of Y-doped Bi_2O_3. It is clear that the sample particles prepared under low temperatures (300 °C and 400 °C) were irregular blocks with particle size of tens to more than one hundred nanometer. Associated with the results of XRD, the particles might be the grains of $Bi_2O_2CO_3$ or the mixture of $Bi_2O_2CO_3$ and β-Bi_2O_3. In contrast, the images of BYO500 and BYO600 display distinctive sheet structures. The thickness of the sheets sizes are 22–27 nm. As previously reported [5], these sheet-shaped crystals are a major phase of α-Bi_2O_3, which is consistent with the XRD results.

Photoabsorptivity: As shown in Fig. 3, the Bi_2O_3 samples doped with low amounts of Y absorbed more visible light than Bi_2O_3. The band gap energy of the BYO samples can be calculated by Eq. (1) [9].

$$(\alpha h\upsilon)^{n/2} = k(h\upsilon - E_g) \quad (1)$$

where α is the absorption coefficient, k is the parameter that is related to the effective masses associated with the valence and conduction bands, n is 4 for an indirect transition, $h\upsilon$ is the absorption energy, and E_g is the band gap energy. Plotting $(\alpha h\upsilon)^2$ versus $h\upsilon$ based on the spectral response in Fig. 3 gave the extrapolated intercept corresponding to the E_g value. The band gaps of BYO200–600 were 2.07, 2.14, 2.00, 1.71, and 1.91 eV (equal to 650 nm), correspondingly. The irregular changes in band gap might be due to the variation in the crystalline phase (Fig. 1) and Y-doping content (see EDX results). For example, $Bi_2O_2CO_3$ and α-Bi_2O_3 with different band gap (2.0 eV and 3.38 eV) [5,15] will exert inverse influences over the electron energy levels and band structures.

Photocatalytic performance: The degradation of 4-chlorophenol under visible light ($\lambda > 420$ nm) was used to test the photocatalytic performance. Nano-TiO_2 (P25) was chosen for comparison. Herein, all photocatalytic reactions followed pseudo-first-order kinetics (Fig. 4). Besides, BYO200–600 presented higher photocatalytic activities than TiO_2. Among them, the BYO600 showed the fastest rate for degradation of 4-chlorophenol during 60 min, six fold improvement over those of BYO200 and BYO300. The rates for BYO200–600 were 0.014, 0.018, 0.0407, 0.079, and 0.0969 min^{-1}, correspondingly.

The benefits of Y-doping have been credited with narrowing energy band gap of photocatalyst [16] and hindering crystallite growth by the surface enriched Y^{3+} [17]. In our case, the hindered crystallite growth was not observed (Fig. 2). Based on our previous studies [10], the Y-doping might distort the lattice and hybridize Y 4d, 5f and Bi 6d orbital energy levels, modifying the electron structure of Bi_2O_3. The photocatalytic activity of BYO200–600 was improved with the increase of annealing temperature and the Y-doping content. Besides, oxygen vacancies and defects might be created during the Y-doping [18] and act as the centers to capture photo-generated electrons and inhibit the recombination of electron–hole pairs. Therefore, the photocatalytic activity of BYO

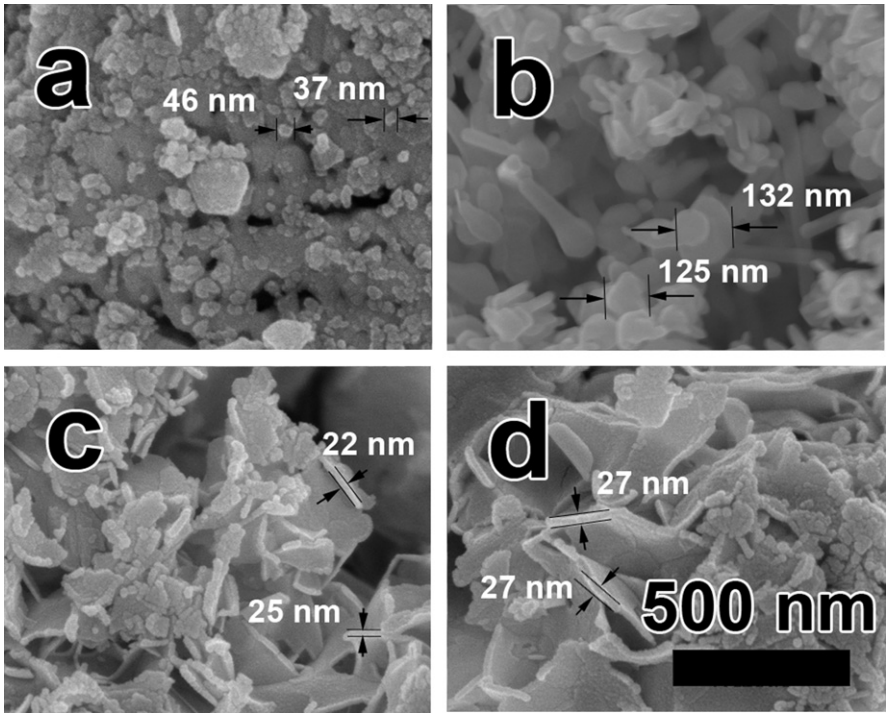

Fig. 2. Scanning electronic microscopy (SEM) images of $Bi_2O_2CO_3$ (annealed at 300 °C), (a) and Y-doped Bi_2O_3 annealed at 400 °C (b), 500 °C (c), and 600 °C (d).

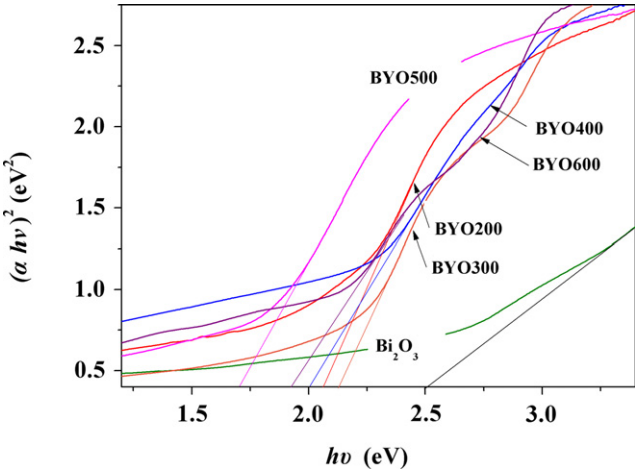

Fig. 3. UV–vis diffuse reflectance spectra (DRS) patterns of TiO_2 (P25), $Bi_2O_2CO_3$ (annealed at 200 °C and 300 °C), Y-doped Bi_2O_3 annealed at 400 °C, 500 °C, and 600 °C.

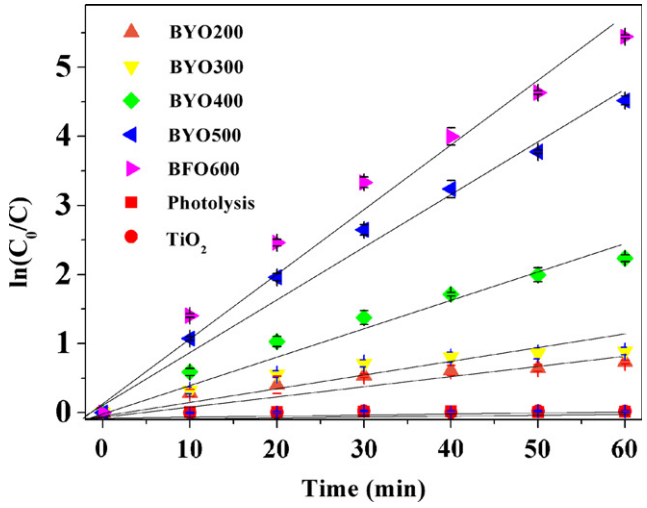

Fig. 4. Kinetics analysis of photocatalytic degradation of 4-chlorophenol by TiO_2 (P25), $Bi_2O_2CO_3$ (annealed at 200 °C and 300 °C), Y-doped Bi_2O_3 annealed at 400 °C, 500 °C, and 600 °C under visible light (> 420 nm).

might be further strengthened by increasing Y-doping content from BYO400 to BYO600 (Fig. 4).

4. Conclusions

In summary, Y-doped Bi_2O_3 samples with different morphology and crystalline phase were prepared, and their photocatalytic properties were evaluated by degrading 4-chlorophenol under visible light irradiation. The results indicated the mixture of β-Bi_2O_3 and $Bi_{15}YO_{24}$ exhibited much higher photocatalytic activities than other samples and TiO_2 (P25), which is mainly ascribed to the Y-induced reconfiguration of the electron structure, the creation of oxygen vacancies and defects.

Acknowledgments

This work was supported by Project 21207004 supported by National Natural Science Foundation of China, special funds of State Key Joint Laboratory of Environment Simulation and Pollution Control (11Y06ESPCN), and National Basic Research Program of China 973 project, (2010CB429003).

References

[1] Fujishima A, Honda K. Nature 1972;238:37–8.
[2] Robertson PKJ, McCullagh C, Skillen N, Adams M. J Chem Technol Biotechnol 2011;86:1002–17.
[3] Guo Y, Shi X, Zhang J, Fang Q, Yang L, Dong F. Mater Lett 2012;86:146–9.

[4] Wu Y, Wang X. Mater Lett 2011;65:2062–5.
[5] Lin G, Tan DZ, Luo FF, Chen DP, Zhao QZ, Qiu JR. J Alloy Compd 2010;507:L43–6.
[6] Cao J, Li X, Lin H, Xu B, Luo B, Chen S. Mater Lett 2012;76:181–3.
[7] Luo JH, Maggard PA. Adv Mater 2006;18:514–7.
[8] Lei YQ, Wang GH, Song SY, Fan WQ, Zhang HJ. CrystEngComm 2009;11: 1857–62.
[9] Wu XH, Qin W, Li L, Guo Y, Xie ZY. Catal Commun 2009;10:600–4.
[10] Yin LF, Niu JF, Shen ZY, Sun Y. Sci China Chem 2010;54:180–5.
[11] Xie JM, Lu XM, Chen M, Zhao GQ, Song YZ, Lu SS. Dyes Pigm 2008;77:43–7.
[12] Zhao D, Peng T, Xiao J, Yan C, Ke X. Mater Lett 2007;61:105–10.
[13] Zhou W, Zhou Y, Tang S. Mater Lett 2005;59:3115–8.
[14] Song M, Bian L, Zhou T, Zhao X. J Rare Earth 2008;26:693–9.
[15] Madhusudan P., Yu J.G., Wang W.G., Cheng B., Liu G. Dalton Trans 2012;41: 14345–53.
[16] Talaat MH, Jamilk KS, Roger GH. Nano 2009;4:225–32.
[17] Atribak I, Bueno-López A, García-García A. J Mol Catal A: Chem 2009;300: 103–10.
[18] Won YJ, Gun DL, Seong SP, Kwon TL. Catal Today 2011;164:395–8.